

## Distribution Agreement

In presenting this thesis or dissertation as a partial fulfillment of the requirements for an advanced degree from Emory University, I hereby grant to Emory University and its agents the non-exclusive license to archive, make accessible, and display my thesis or dissertation in whole or in part in all forms of media, now or hereafter known, including display on the world wide web. I understand that I may select some access restrictions as part of the online submission of this thesis or dissertation. I retain all ownership rights to the copyright of the thesis or dissertation. I also retain the right to use in future works (such as articles or books) all or part of this thesis or dissertation.

Signature:



Chenxi Du

10/04/2023  
Date

Investigation of predictability of photo images from different anatomic regions for  
detecting anemia among preterm infants

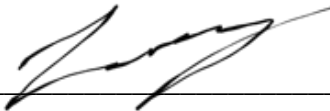
By

Chenxi Du  
Master of Public Health

Department of Biostatistics and Bioinformatics

---

Amita Manatunga, PhD  
(Thesis Advisor)



---

Jeong Hoon Jang, PhD  
(Reader)

Investigation of predictability of photo images from different anatomic regions for  
detecting anemia among preterm infants

By

Chenxi Du

B.S., Renmin University of China, 2016

Thesis Committee Chair: Amita Manatunga, PhD

An abstract of  
A thesis submitted to the Faculty of the  
Rollins School of Public Health of Emory University  
in partial fulfillment of the requirements for the degree of  
Master of Public Health  
in Biostatistics  
2022

## Abstract

### Investigation of predictability of photo images from different anatomic regions for detecting anemia among preterm infants

By Chenxi Du

**Background:** Anemia is a global health issue affecting people of all ages, with the highest prevalence among preschool-age children. Traditional diagnosis methods for neonatal anemia involve frequent blood sampling, which can lead to blood loss-induced anemia and the development of complications. Therefore, a non-invasive method for diagnosing anemia for preterm infants is needed. One potential solution is developing a smartphone application that captures videos and images through the camera and predicts Hgb levels based on RGB values. Several smartphone applications have been developed for monitoring hemoglobin levels in adults, but there is no evidence regarding their efficacy in infants.

**Objective:** The purpose of this study is to develop a method for predicting neonatal anemia among preterm infants using RGB values and metadata extracted from smartphone images of various body regions, including the fingernail, toenail, and palm. Furthermore, we aim to determine which body region that can predict anemia with better degree of accuracy.

**Method:** PCA was conducted on RGB data extracted from body region images for dimension reduction. Four logistic regression models were built to examine for the best region for predicting anemia. Stepwise model selection was employed to select the proper predictors among image metadata (PCs of RGB value, brightness value, exposure time) and infants' demographic data (age, gender, race, ethnicity, birth weight, and gestational age). Cross-validation was used to test accuracy and AUC is the main criterion.

**Result:** 65 infants and 1000 images from 6 body regions were included in the analysis. Principal component analysis was used to include image data in the models, and four principal components were selected. Logistic regressions were fitted separately for the whole dataset and regional datasets. The Palm model reported the highest AUC comparing with all other models with cross validation AUC as 0.726, while the Fingernail Model has the lowest AUC (0.663).

**Conclusion:** The palm region images gave a slightly better result comparing with other anatomic regions. However, in practice, there are difficulties for nurses taking pictures in this vulnerable population. Given that there is no large difference in the AUC, in practice, any region can be chosen.

Investigation of predictability of photo images from different anatomic regions for  
detecting anemia among preterm infants

By

Chenxi Du

B.S., Renmin University of China, 2016

Thesis Committee Chair: Amita Manatunga, PhD

An abstract of  
A thesis submitted to the Faculty of the  
Rollins School of Public Health of Emory University  
in partial fulfillment of the requirements for the degree of  
Master of Public Health  
in Biostatistics  
2022

# Table of Contents

<b>1. Introduction.....</b>	<b>1</b>
<b>2. Method .....</b>	<b>4</b>
2.1 Data Source.....	4
2.1.1 Cohort Selection.....	4
2.1.2 Image Data Collection .....	4
2.2 Statistical Analysis.....	6
2.2.1 Principal Component Analysis.....	6
2.2.2 Logistic Regression Model .....	7
<b>3. Result.....</b>	<b>9</b>
3.1 Preliminary Analysis.....	9
3.2 Prediction results.....	10
<b>4. Discussion.....</b>	<b>13</b>
<b>5. Tables:.....</b>	<b>15</b>
<b>6. Appendix:.....</b>	<b>24</b>
<b>7. Reference: .....</b>	<b>26</b>

## 1. Introduction

Anemia is a significant global health issue that affects individuals across various regions, age groups, and genders. According to the World Health Organization (WHO), approximately 1.62 billion people worldwide (24.8% of the global population) are affected by anemia [1]. The prevalence of anemia is highest among preschool-age children, with 47.4% affected [1]. Anemia can have a severe impact on neonates if left untreated [2]. Neonatal anemia can result in reduced oxygen-carrying capacity of the blood, leading to hypoxia, tissue damage and complications such as respiratory distress, developmental delays, impaired cognitive function, and even death in severe cases [3]. Traditional diagnosis methods for neonatal anemia include blood tests such as hemoglobin (Hgb) and hematocrit, complete blood count (CBC), peripheral smear, and iron studies. However, frequent blood sampling for diagnosis can lead to blood loss-induced anemia and the development of both Necrotizing Enterocolitis (NEC) and Bronchopulmonary dysplasia (BPD) [4]. Besides, preterm infants' hematopoietic system is underdeveloped [11], thus frequent blood draw can cause much severe consequences comparing with infants with normal gestational age. Therefore, there is a need for a non-invasive method for diagnosing anemia for preterm infants. Such a method would be a valuable addition to clinical diagnosis, as it would reduce the risks associated with frequent blood sampling, while providing accurate and reliable results for neonatal anemia diagnosis.

Traditional physical diagnosis considers pallor of the conjunctivae, nail beds, face, palms as signs for anemia [10]. Pallor can be easily identified with color intensity drawn from image of these anatomic regions. RGB value, which indicates red, green, and blue intensity, is one of the widely indices to quantify color intensity and could thus be adopted as an index to evaluate hemoglobin level accordingly. Therefore, developing a smartphone application that captures

videos and images of relevant anatomic regions through the camera, extract their RGB values, and predicts Hgb levels based on these values could be a non-invasive method for anemia diagnosis.

Smartphone has been proved to be an efficient device for heart rate monitoring [5], ophthalmopathy diagnosis [6], skin diagnosis [6], and telemedicine. In addition, several smartphone applications have been developed for monitoring hemoglobin levels.

One such application is HemaApp (Wang et al, 2016), which utilizes the smartphone's camera to monitor blood hemoglobin concentration in patients ranging from 6 to 77 years of age [7]. The application records a 15-second RGB video, which is then analyzed using both SVM regression and linear regression models to calculate the hemoglobin level and detect anemia. The hemoglobin concentration estimated by HemaApp yields a 0.82 Spearman correlation with CBC Hgb level (gold standard), with a sensitivity and precision of 0.857 and 0.765 of predicting anemia, respectively. Mannino et al (2018) developed another application for predicting Hgb level and detecting anemia among adult patients based on their fingernail images[8]. The algorithm of this application uses a robust multi-linear regression model with bisquare weighting, which includes average RGB value and image metadata as predictor variables. The study reported MAE (mean absolute error) of 0.82 between its predictions and the CBC Hgb levels, suggesting that the application may provide promising result for monitoring hemoglobin concentration on adults.

It is worth noting that previous studies have primarily focused on adult populations, and there is no known study on the efficacy of current smartphone applications for monitoring hemoglobin levels in infants. Besides, preterm infants are more likely to be anemic compared to healthy infants, and frequent blood draw can cause more severe consequences [12]. Additionally, due to



their smaller fingernail size, it may be more challenging to extract accurate image data from the fingernail region in infants. Therefore, the development of an algorithm specifically designed for preterm infants is necessary, and alternative photograph body regions other than the fingernail should be considered to improve accuracy and reliability.

The purpose of this study is to develop a method for predicting neonatal anemia among preterm infants using RGB values and metadata extracted from smartphone images of various anatomic regions, including the fingernail, toenail, and palm. Furthermore, we aim to determine which body region predicts anemia with better degree of accuracy.

## **2. Method**

### **2.1 Data Source**

#### **2.1.1 Cohort Selection**

The infant cohort was recruited by Dr. Cassandra Josephson at Emory University for a prospective, multicenter, observational birth-cohort study focusing on the effects of red blood cell transfusion on digestive tract oxygenation in preterm infants. Preterm infants (gestational week < 37 weeks) at 3 level III neonatal intensive care units (NICUs) in Atlanta are eligible to participate in the study. The hospitals with NICUs in Atlanta are Grady Memorial Hospital, Emory University Hospital Midtown, and Northside Hospital, in which the first two are academically affiliated.

The study obtained written consent from the parents or legal guardians of the infants before they could participate in the research. Infants with birthweight greater than 1250 grams and postnatal age greater than 7 days were excluded. Infants were also excluded if they were unlikely to survive past 7 days, had severe congenital abnormality, had received transfusion before enrollment, or if their mothers decided not to participate.

Until March 15, 2023, 66 eligible infants were enrolled in the study. All enrolled infants were followed for 90 days or until they were discharged from hospital, transfer to another hospital, or death. Their demographic data (including age, gender, race, ethnicity, gestational age, and so on) were collected upon enrollment. Their hemoglobin levels were monitored and recorded through a weekly blood test, along with the test date.

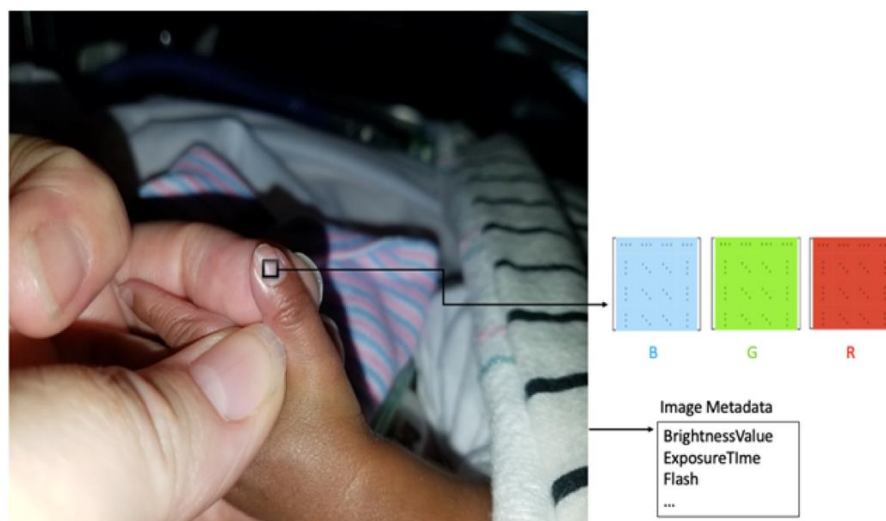
#### **2.1.2 Image Data Collection**

A Samsung S21 model was used to collect photos from different anatomic regions (left fingernail, right fingernail, left toenail, right toenail, left palm, right palm) of each enrolled

infant, with default camera settings, auto-focus and adjust brightness by tapping on the focus region chose by nurses. The photos were taken at a shooting distance of 0.5 meters from the target region, adjusted by nurses. The pictures were captured in consistent lighting conditions and stable illumination. The picture time was within 24 hours of the Hgb blood test date, so theoretically, each picture is attached with a corresponding CBC Hgb level. It is worth noticing that, not all body regions were pictured, limited regions were selected based on nurses' convenience.

After all the pictures were collected, each image was manually processed using the MATLAB code, which is the same code as that used in AnemoCheck Mobile App developed by Dr. Robert Mannio. Then, on a rectangle region was selected for each image, three  $51 \times 51$  pixel matrices that contain RGB (red, green, blue) color intensity values were generated, along with the imagemeta variables including brightness value and exposure time (Figure 1). Each of the  $51 \times 51$  pixel matrices of RGB values was converted to a 2601-dimensional vector. To achieve consistency and retain interpretability of the converted RGB vectors across different subjects, their elements were rearranged in a descending order based on the red color intensity.

**Figure 1.** Sample image for demonstrate the process of extracting RGB value and image meta data.



To examine the data reproducibility, two other image data processors are included to process a same subset of images (N=71). Concordance Correlation Coefficient (CCC) and Intraclass Correlation Coefficient (ICC) was calculated pairwise between three processors on RGB (red, green, blue) vectors separately to evaluate reproducibility of pixel specified intensity. Estimated CCC and ICC were all relatively high, indicating high agreement across processors (Table A.1 in Appendix).

## 2.2 Statistical Analysis

### 2.2.1 Principal Component Analysis

Principal component analysis was applied to RGB vectors after combining all the RGB values.

Consider a dataset with  $n$  observations and  $p$  numerical variables, which can define a  $n \times p$  data matrix  $\mathbf{X}$ . We want to find a set of linear combination of the columns of matrix  $\mathbf{X}$  that can account for most of the variance in  $\mathbf{X}$ . The linear combination can be written as  $\mathbf{X}\mathbf{a}$ , while weight matrix  $\mathbf{a}$  has a dimension of  $p \times p$ , or define as a  $p$ -dimensional vectors  $a_1, \dots, a_p$ .  $\mathbf{X}\mathbf{a}_j$  is considered as  $j$ th principal component (PC).

To find the weight matrix  $\mathbf{a}$ , the variance-covariance matrix of across  $p$  numerical variables is needed, as follows:

$$\begin{bmatrix} \text{Var}(X_1) & \cdots & \text{Cov}(X_1, X_p) \\ \vdots & \ddots & \vdots \\ \text{Cov}(X_p, X_1) & \cdots & \text{Var}(X_p) \end{bmatrix}$$

The corresponding eigenvectors of the variance-covariance matrix is the weight matrix  $\mathbf{a}$ . The eigenvector with the highest eigenvalue is the principal component that captures the most significant amount of variance in  $\mathbf{X}$ . By sorting the eigenvalues in descending order, we can determine the percentage of variance explained by each principal component, which is calculated

as the ratio of the eigenvalue to the sum of all eigenvalues. We can select the first few eigenvectors with the largest eigenvalues and use them to calculate the principal components. These components can account for most of the data variation while having a lower dimension than the original dataset.

### **2.2.2 Logistic Regression Model**

After selecting the proper numbers of PCs for the RGB variables, multiple logistic regression models were built using the derived PC scores to predict the binary anemia outcome (1 = anemia; 0 = no anemia).

In the study, infants with CBC Hgb levels lower than 10 g/dL were classified as anemic [9]. In addition to the PC scores that represent the RGB values, other potential covariates were also considered for inclusion in the logistic regression models, including image metadata (brightness value and exposure time) and demographic data (age, gender, race, ethnicity, birth weight, and gestational age). Gender, race, and ethnicity were treated as categorical variables, while the other demographic variables (age, birth weight and gestational age) were included as continuous variables. To maintain consistency in scale with the other continuous variables, exposure time was rescaled by a factor of 10,000. Stepwise variable selection was used to choose the best prediction model based on AIC as the selection criterion.

To evaluate images from which body region can better represent infants' anemia condition, logistic regression models for different body regions were built. The regression models were built based on different dataset: whole dataset, fingernail photos only, toenail photos only, and palm photos only. The four logistic regression models can be referred as Whole Model, Fingernail Model, Toenail Model, and Palm Model respectively. Aside from all the potential covariates mentioned previously, the Whole Model also include body regions as one of the

potential predictors. Stepwise model selection process for each model was conducted separately using the dataset. K-fold cross-validation was employed to evaluate the accuracy of the models with AUC (Area Under the ROC curve) as evaluation criterion. Due to limited sample size, splitting data method was not employed to build and evaluate the model.

### 3. Result

#### 3.1 Preliminary Analysis

By March 15, 2023, 66 infants were enrolled in the study with corresponding 1065 photos collected. Given the problem that several image data are missing when CBC Hgb levels were measured, and the CBC Hgb values are missing for some photos, only 65 infants and 1000 images across 6 body regions (left fingernail, right fingernail, left toenail, right toenail, left palm, right palm) were included in the analysis. On average, each infant had 15.4 pictures taken (with a standard deviation of 8.5) (Table 2). Fingernail is the body region that got the most photos taken with 415 pictures for 65 infants across time (41.5%), followed by palm with 395 pictures for 64 infants (39.5%) and toenail with 190 images for 59 infants (19.0%) (Table 2).

Regarding the demographic information, gender, ethnicity, race, age (week), birth weight (g), and gestational age (week) were summarized and considered to be included in the models. On the individual level, the majority of infants are female (63.1%), and Hispanic participants are scarce with only 6 infants included (9.2%). All the infants had low birth weight (maximum 1240 grams) and were premature (maximum gestational age 31 weeks) (Table 1). 268 times CBC Hgb measurements from 33 infants were tested as anemia. The average proportion of getting test as anemia across time for each infants was 24.3% with standard deviance as 30.5% (Table 2).

Univariate analysis was performed to preliminarily examine the association between demographic covariates and anemia without adjustment of any other variables. For the dataset that includes all images, age (p-value<0.001), gender (p-value<0.001), race (p-value<0.001), birth weight (p-value<0.001) and gestational age (week) (p-value<0.001) all showed a significant relationship with anemia (Table 3). For the dataset that only includes pictures taken from fingernails, gender, race, age and gestational age (week) showed significance (Table 4.1). For the

dataset only includes pictures taken from toenails, only age and birth weight showed a significant association with anemia (Table 4.2). For the dataset that only includes palm region pictures, race, gender, age and gestational age (week) showed an association with anemia outcome (Table 4.3).

To include image data in the models, was performed on RGB vector data. The first four PCs explained 98.24% of the variance of the original RGB dataset, with PC1 explaining 80.53% of the variance, PC2 explaining 13.18%, PC3 explaining 2.53%, and PC4 explaining 2.00% (Figure A.1 in Appendix). The variance explained by the first four PCs are reasonably large (98.24%). Thus, the PCs can be good representative for RGB values, and the corresponding PC scores were included in the models as predictors along with brightness value and exposure time.

RGB PC scores showed significant association with anemia in whole dataset, fingernail dataset and palm dataset, while in toenail dataset, RGB PC scores were marginally significant association with outcome (Table 3, Table 4.1-4.3). Besides, brightness value and exposure time were also significantly associated with anemia in all datasets (Table 3, Table 4.1-4.3).

### **3.2 Prediction results**

After eliminating missing values, four logistic regressions were fitted separately using whole dataset and regional datasets (fingernail dataset, toenail dataset and palm dataset), with outcome as anemia (CBC Hgb < 10 g/dL), and covariates were selected using stepwise model selection method.

The Whole Model built on full dataset (N=874) included PC scores of RGB value, gender, race, age, gestational age, brightness value, exposure time, and body region as covariates (Table 5.1). AUC for the Whole Model was 0.721. The Fingernail Model built on fingernail photos only (N=357) included PCs of RGB value, gender, race, age, gestational age, brightness value, and exposure time as covariates (Table 5.2). The corresponding AUC for Fingernail Model was



0.717. While the PC scores for RGB showed a significant association with outcome in Fingernail data when evaluated independently, the PCs turned to have marginal significant association with anemia (p-value=0.057) after adjusted for other covariates. The Toenail Model built based on toenail images only (N=175) included PC scores of RGB values, race, birth weight and brightness value only (Table 5.3), while the AUC for Toenail Model was 0.784. In contrast to Fingernail Model, after adjusting for covariates, the association between PC scores of RGB value became significant in Toenail Model (p-value<0.001). The Palm Model built based on palm images only (N=342) included PCs of RGB values, gender, race, gestational age, and exposure time (Table 5.4). The AUC for Palm Model was 0.760. The association between anemia and RGB PC scores kept consistent for univariate analysis and multivariate analysis (both p-value<0.001). The predicted probabilities of having anemia calculated with above four models showed some but not perfect separation between anemia group and healthy group (Figure A.2 in Appendix).

After selected out the proper covariates for the four logistic regression models (Whole Model, Fingernail Model, Toenail Model, Palm Model), 5-fold cross-validation was conducted on all the models to evaluate the prediction accuracy on anemia. The results were summarized in Table 6. Overall, the four models all show reasonably high prediction accuracy. The Palm model reported the highest AUC comparing with all other models with cross validation AUC as 0.726, while the Fingernail Model has the lowest AUC (0.663).

To evaluate the capability of image data, models without image variables were fit. Comparing with the models without image variables (brightness value, exposure time, and PC scores of RGB values) included, all four model with image variable included show improvement in AUC, which suggests that the image data helps to improve the prediction models. The Palm

Model also has the highest improvement on AUC (from 0.603 to 0.726) comparing with the model without image data. Thus, palm images can give a relatively better prediction on anemia among preterm infants comparing with other body regions (fingernail or toenail) in this study.

## 4. Discussion

In this study, several logistic regression models were fit to predict anemia based on images taken from preterm infants' anatomic regions. The primary predictor of interest is the RGB values extracted from photos. principal component analysis was conducted on RGB values to reduce dimension and four PCs were selected to account for 98.24% of the data variation. Four logistic regression models building on fingernail images, toenail images, and palm images were fit. AUC (Area Under the ROC curve) was calculated after cross validation to evaluate the prediction performance.

Overall, all the models had relatively good prediction on anemia. All four models produced high AUC value under 5-fold cross validation, with Palm Model had the highest AUC (0.726) and Fingernail Model had the lowest AUC (0.663). The palm region images gave a slightly better result comparing with other anatomic regions. Thus, the palm may be the best region to take photos for prediction anemia among preterm infants according to the result. But this accuracy difference may be minimal. In practice, there are difficulties for nurses taking pictures in this vulnerable population, including hard to focus, hard to select the color region. Given that there is no large difference in the AUC, in practice, any region can be chosen.

Although the study results look promising, there are several limitations that need further examine. First of all, since the dataset is inherently longitudinal, the current logistic regressions analysis does not account for the potential correlation due to the repeated measurements of the same infants. Fail to count for correlation can lead to variation increase in prediction outcome. Thus, in the future study, mixed-effect models can be considered to adjust for the correlation. Besides, as the dataset is relatively small, current study did not have test samples to examine for evaluating the prediction models. Even though cross-validation was conducted for evaluation,

the applicability of employing current model on new data is still unknown. And also the images from different anatomic regions are unbalanced, the model built on smaller dataset could be less trained. Recruiting more eligible participants and balancing the images distribution by taking photo on every anatomic regions for each infants can greatly help to improve prediction results. Furthermore, currently principal component analysis method does not take the spatial association among RGB values into account. A high dimensional principal component analysis method would be desired for RGB value dimension reduction.

## 5. Tables:

**Table 1.** Descriptive statistics of demographic information for enrolled infants (n=65).

	<b>Overall (n=65)</b>
<b>Gender</b>	
Male	24 (36.9%)
Female	41 (63.1%)
<b>Ethnicity</b>	
Yes	6 (9.23%)
No	59 (90.8%)
<b>Race</b>	
White	26 (49.1%)
Black	20 (37.7%)
Other	7 (13.2%)
<i>Missing</i>	<i>12</i>
<b>Age (week)</b>	
Mean (SD)	2.31 (1.79)
Median [Min, Max]	2.00 [0, 8.00]
<b>Birth Weight</b>	
Mean (SD)	905 (212)
Median [Min, Max]	890 [406, 1240]
<b>Gestational Age (week)</b>	
Mean (SD)	27.4 (2.09)
Median [Min, Max]	27.0 [22.0, 31.0]

\* n indicates number of infants.

**Table 2.** Descriptive statistics of number of pictures taken for each infants (n=65).

	<b>All pictures</b>	<b>Fingernail pictures</b>	<b>Palm pictures</b>	<b>Toenail pictures</b>
<b>Number of infants with certain regional pictures</b>	<b>(n=65)</b>	<b>(n=65)</b>	<b>(n=64)</b>	<b>(n=59)</b>
<b>Number of pictures</b>				
Mean (SD)	15.4 (8.54)	6.38 (3.53)	6.17 (3.43)	3.22 (1.96)
Median [Min, Max]	15.0 [1.00, 32.0]	6.00 [1.00, 15.0]	6.00 [1.00, 13.0]	3.00 [1.00, 8.00]
<b>Probability of developing anemia (%)</b>				
Mean (SD)	24.3 (30.5)	-	-	-
Median [Min, Max]	9.38 [0, 100]	-	-	-

\* n indicates number of infants.

**Table 3.** Descriptive statistics of demographic information and image data for overall pictures (N=1000).

	<b>Overall (N=1000)</b>	<b>Anemia (N=268)</b>	<b>No Anemia (N=732)</b>	<b>P-value</b>
<b>Demographic Variables</b>				
<b>Gender</b>				<b>&lt; 0.001</b>
Male	379 (37.9%)	75 (28.0%)	304 (41.5%)	
Female	621 (62.1%)	193 (72.0%)	428 (58.5%)	
<b>Ethnicity</b>				0.699
Yes	113 (11.3%)	32 (11.9%)	81 (11.1%)	
No	887 (88.7%)	236 (88.1%)	651 (88.9%)	
<b>Race</b>				<b>&lt; 0.001</b>
White	476 (54.5%)	97 (41.8%)	379 (59.0%)	
Black	299 (34.2%)	105 (45.3%)	194 (30.2%)	
Other	99 (11.3%)	30 (12.9%)	69 (10.7%)	
<i>Missing</i>	<i>126</i>	<i>36</i>	<i>90</i>	
<b>Age (week)</b>				<b>&lt; 0.001</b>
Median [Q1, Q3]	5.00 [2.00, 8.00]	6.00 [4.00, 8.25]	4.00 [2.00, 8.00]	
<b>Birth Weight (g)</b>				<b>&lt; 0.001</b>
Median [Q1, Q3]	860 [694, 1080]	815 [694, 1070]	890 [739, 1080]	
<b>Gestational Age (week)</b>				<b>&lt; 0.001</b>
Median [Q1, Q3]	27.0 [26.0, 28.0]	26.0 [25.0, 28.0]	27.0 [26.0, 28.0]	
<b>Image Meta Data</b>				
<b>Brightness Value</b>				<b>&lt; 0.001</b>
Median [Q1, Q3]	7.57 [6.71, 8.21]	7.83 [7.12, 8.36]	7.47 [6.59, 8.11]	
<b>Exposure Time (<math>\times 10^{-4}</math> s)</b>				<b>&lt; 0.001</b>
Median [Q1, Q3]	8.45 [5.42, 15.4]	7.05 [4.88, 11.5]	9.14 [5.81, 16.7]	
<b>RGB Principal Component</b>				<b>&lt; 0.001</b>
PC1	0.591 [-53.1, 54.6]	-10.9 [-54.2, 40.6]	7.64 [-51.2, 59.8]	
PC2	-3.24 [-21.8, 15.6]	-6.93 [-26.7, 11.8]	-1.81 [-19.6, 15.9]	
PC3	3.55 [-5.85, 9.64]	4.43 [-3.20, 10.6]	2.67 [-7.02, 9.21]	
PC4	0.444 [-7.20, 8.17]	-1.98 [-8.35, 3.81]	1.42 [-6.98, 9.55]	

\* N indicates number of observations.

\* P-values were calculated using Chi-square test for categorical variables; Wilcoxon rank sum test for continuous variables.

\* P-value for PCs was calculated using likelihood ratio test

**Table 4.1.** Descriptive statistics of demographic information and image data for fingernail pictures only (N=415).

	Fingernail Photos N=415		P-value
	Anemia (N=44)	No Anemia (N=371)	
<b>Demographic Variables</b>			
<b>Gender</b>			<b>0.016</b>
Male	31 (27.0%)	119 (39.7%)	
Female	84 (73.0%)	181 (60.3%)	
<b>Ethnicity</b>			0.774
Yes	13 (11.3%)	31 (10.3%)	
No	102 (88.7%)	269 (89.7%)	
<b>Race</b>			<b>0.012</b>
White	40 (41.7%)	153 (58.6%)	
Black	45 (46.9%)	81 (31.0%)	
Other	11 (11.5%)	27 (10.3%)	
Missing	19	39	
<b>Age (week)</b>			<b>&lt; 0.001</b>
Median [Q1, Q3]	6.00 [4.00, 8.00]	4.00 [2.00, 8.00]	
<b>Birth Weight (g)</b>			0.080
Median [Q1, Q3]	815 [694, 1070]	879 [699, 1080]	
<b>Gestational Age (week)</b>			<b>&lt; 0.001</b>
Median [Q1, Q3]	26.0 [25.0, 28.0]	27.0 [26.0, 28.0]	
<b>Image Meta Data</b>			
<b>Brightness Value</b>			<b>0.002</b>
Median [Q1, Q3]	7.80 [6.85, 8.42]	7.34 [6.55, 8.03]	
<b>Exposure Time (<math>\times 10^{-4}</math> s)</b>			<b>0.002</b>
Median [Q1, Q3]	7.18 [4.66, 13.9]	9.92 [6.15, 17.2]	
<b>RGB Principal Component</b>			<b>&lt; 0.001</b>
PC1	-19.5 [-70.2, 28.5]	-19.8 [-69.8, 38.6]	
PC2	-18.5 [-31.5, 3.56]	-9.90 [-26.6, 5.92]	
PC3	0.598 [-7.73, 7.70]	-1.85 [-13.9, 6.91]	
PC4	-3.17 [-11.3, 3.58]	-0.208 [-8.93, 7.83]	

\* N indicates number of observations.

\* P-values were calculated using Chi-square test for categorical variables; Wilcoxon rank sum test for continuous variables.

\* P-value for PCs was calculated using likelihood ratio test



**Table 4.2.** Descriptive statistics of demographic information and image data for toenail pictures only (N=190).

	Toenail Photos N=190		P-value
	Anemia (N=46)	No Anemia (N=144)	
<b>Demographic Variables</b>			
<b>Gender</b>			0.069
Male	15 (32.6%)	69 (47.9%)	
Female	31 (67.4%)	75 (52.1%)	
<b>Ethnicity</b>			0.768
Yes	5 (10.9%)	18 (12.5%)	
No	41 (89.1%)	126 (87.5%)	
<b>Race</b>			0.079
White	17 (39.5%)	78 (59.1%)	
Black	18 (41.9%)	39 (29.5%)	
Other	8 (18.6%)	15 (11.4%)	
Missing	3	12	
<b>Age (week)</b>			<b>0.006</b>
Median [Q1, Q3]	6.00 [4.00, 8.00]	4.00 [2.00, 8.00]	
<b>Birth Weight (g)</b>			<b>0.005</b>
Median [Q1, Q3]	739 [693, 977]	954 [790, 1080]	
<b>Gestational Age (week)</b>			0.092
Median [Q1, Q3]	26.5 [25.0, 28.0]	27.0 [26.0, 28.0]	
<b>Image Meta Data</b>			
<b>Brightness Value</b>			<b>0.021</b>
Median [Q1, Q3]	8.05 [7.60, 8.38]	7.68 [6.96, 8.41]	
<b>Exposure Time (<math>\times 10^{-4}</math> s)</b>			<b>0.021</b>
Median [Q1, Q3]	6.07 [4.83, 8.29]	7.81 [4.69, 12.8]	
<b>RGB Principal Component</b>			0.089
PC1	-12.9 [-54.9, 40.2]	-0.629 [-66.5, 57.7]	
PC2	-23.5 [-38.5, 6.64]	-8.66 [-24.8, 14.0]	
PC3	3.81 [-5.15, 9.71]	0.280 [-6.21, 6.79]	
PC4	-2.80 [-9.38, 3.46]	0.342 [-8.28, 7.74]	

\* N indicates number of observations.

\* P-values were calculated using Chi-square test for categorical variables; Wilcoxon rank sum test for continuous variables.

\* P-value for PCs was calculated using likelihood ratio test

**Table 4.3.** Descriptive statistics of demographic information and image data for palm pictures only (N=395).

	Palm Photos N=395		P-value
	Anemia (N=107)	No Anemia (N=288)	
<b>Demographic Variables</b>			
<b>Gender</b>			<b>0.016</b>
Male	29 (27.1%)	116 (40.3%)	
Female	78 (72.9%)	172 (59.7%)	
<b>Ethnicity</b>			0.587
Yes	14 (13.1%)	32 (11.1%)	
No	93 (86.9%)	256 (88.9%)	
<b>Race</b>			<b>0.017</b>
White	40 (43.0%)	148 (59.4%)	
Black	42 (45.2%)	74 (29.7%)	
Other	11 (11.8%)	27 (10.8%)	
Missing	14	39	
<b>Age (week)</b>			<b>&lt; 0.001</b>
Median [Q1, Q3]	7.00 [4.00, 9.00]	4.00 [2.00, 8.00]	
<b>Birth Weight (g)</b>			0.166
Median [Q1, Q3]	825 [694, 1070]	890 [729, 1080]	
<b>Gestational Age (week)</b>			<b>&lt; 0.001</b>
Median [Q1, Q3]	26.0 [26.0, 28.0]	27.0 [26.0, 28.0]	
<b>Image Meta Data</b>			
<b>Brightness Value</b>			<b>0.005</b>
Median [Q1, Q3]	7.63 [7.10, 8.32]	7.43 [6.52, 8.07]	
<b>Exposure Time (<math>\times 10^{-4}</math> s)</b>			<b>0.003</b>
Median [Q1, Q3]	8.06 [5.02, 11.7]	9.58 [5.95, 17.6]	
<b>RGB Principal Component</b>			<b>&lt; 0.001</b>
PC1	-3.19 [-36.4, 50.3]	25.4 [-20.2, 75.5]	
PC2	3.32 [-10.1, 22.8]	10.1 [-5.01, 22.6]	
PC3	8.69 [3.85, 12.2]	6.95 [0.203, 11.8]	
PC4	0.184 [-5.73, 4.57]	4.34 [-3.19, 11.2]	

\* N indicates number of observations.

\* P-values were calculated using Chi-square test for categorical variables; Wilcoxon rank sum test for continuous variables.

\* P-value for PCs was calculated using likelihood ratio test

**Table 5.1.** Logistic regression model built based on all photos (Whole Model) using stepwise model selection method (N=874).

	Coefficients Estimator	95% Confidence Interval	P-value
Intercept	3.218	(-0.739, 7.197)	0.110
RGB PC1	0.004	(0.002, 0.006)	<b>0.001</b>
RGB PC2	0.001	(-0.005, 0.006)	0.803
RGB PC3	-0.002	(-0.018, 0.013)	0.773
RGB PC4	0.024	(0.009, 0.038)	<b>0.001</b>
Gender (ref: Male)			
Female	-0.501	(-0.857, -0.151)	<b>0.005</b>
Race (ref: White)			
Black	-0.689	(-1.052, -0.328)	< <b>0.001</b>
Other	-0.734	(-1.25, -0.205)	<b>0.006</b>
Age (week)	-0.055	(-0.107, -0.004)	<b>0.035</b>
Gestational Age (week)	0.159	(0.056, 0.263)	<b>0.003</b>
Brightness Value	-0.678	(-1.008, -0.351)	< <b>0.001</b>
Exposure Time (*10 <sup>-4</sup> s)	-0.025	(-0.052, 0.003)	<b>0.045</b>
Body Region (ref: Fingernail)			
Toenail	0.192	(-0.257, 0.652)	0.406
Palm	-0.339	(-0.768, 0.087)	0.120

\* N indicates number of observations.

**Table 5.2.** Logistic regression model built based on fingernail photos only (Fingernail Model) using stepwise model selection method (N=357).

	Coefficients Estimator	95% Confidence Interval	P-value
Intercept	4.172	(-2.394, 11.901)	0.250
RGB PC1	0.001	(-0.003, 0.005)	0.490
RGB PC2	0.001	(-0.008, 0.01)	0.795
RGB PC3	-0.004	(-0.026, 0.017)	0.702
RGB PC4	0.019	(-0.001, 0.04)	0.063
Gender (ref: Male)			
Female	-0.460	(-1.03, 0.094)	0.107
Race (ref: White)			
Black	-0.624	(-1.194, -0.056)	<b>0.031</b>
Other	-0.593	(-1.418, 0.278)	0.167
Age (week)	-0.068	(-0.149, 0.013)	0.097
Gestational Age (week)	0.174	(0.011, 0.341)	<b>0.038</b>
Brightness Value	-0.834	(-1.544, -0.289)	<b>0.009</b>
Exposure Time (*10 <sup>-4</sup> s)	-0.047	(-0.118, -0.008)	0.118

\* N indicates number of observations.

**Table 5.3.** Logistic regression model built based on toenail photos only (Toenail Model) using stepwise model selection method (N=175).

	Coefficients Estimator	95% Confidence Interval	P-value
Intercept	4.995	(0.391, 9.89)	<b>0.038</b>
RGB PC1	0.007	(0.002, 0.013)	<b>0.015</b>
RGB PC2	0.007	(-0.005, 0.02)	0.244
RGB PC3	0.017	(-0.025, 0.06)	0.414
RGB PC4	0.019	(-0.015, 0.054)	0.281
Race (ref: White)			
Black	-0.875	(-1.739, -0.034)	<b>0.043</b>
Other	-1.780	(-3.02, -0.577)	<b>0.004</b>
Birth weight	0.004	(0.002, 0.006)	<b>0.001</b>
Brightness Value	-0.828	(-1.435, -0.265)	<b>0.005</b>

\* N indicates number of observations.

**Table 5.4.** Logistic regression model built based on palm photos only (Palm Model) using stepwise model selection method (N=342).

	Coefficients Estimator	95% Confidence Interval	P-value
Intercept	-5.414	(-10.079, -0.925)	<b>0.020</b>
RGB PC1	0.008	(0.004, 0.012)	<b>&lt;0.001</b>
RGB PC2	0.001	(-0.008, 0.01)	0.818
RGB PC3	-0.013	(-0.044, 0.014)	0.368
RGB PC4	0.040	(0.013, 0.069)	<b>0.005</b>
Gender (ref: Male)			
Female	-0.556	(-1.133, 0.005)	0.055
Race (ref: White)			
Black	-0.915	(-1.53, -0.311)	<b>0.003</b>
Other	-0.873	(-1.745, 0.032)	0.052
Gestational Age (week)	0.232	(0.07, 0.401)	<b>0.006</b>
Exposure Time (*10 <sup>-4</sup> s)	0.067	(0.031, 0.108)	<b>0.001</b>

\* N indicates number of observations.

**Table 6.** Prediction accuracy evaluated for Whole Model, Fingernail Model, Toenail Model, Palm Model using 5-fold cross validation.

	AUC	AUC without Image variables included
Whole Model	0.698 (0.043)	0.636 (0.051)
Fingernail Model	0.663 (0.072)	0.626 (0.075)
Toenail Model	0.721 (0.063)	0.627 (0.080)
Palm Model	0.726 (0.061)	0.603 (0.076)

\*Report as Estimator (standard deviance)

## 6. Appendix:

**Table A. 1.** Descriptive statistics for CCC and ICC for pairwise processors (N=71).

	<b>Processor 1 &amp; Processor 2</b>	<b>Processor 1 &amp; Processor 3</b>	<b>Processor 2 &amp; Processor 3</b>
<b>Coefficient of Concordance (CCC)</b>			
Red	0.95 [0.94, 0.96]	0.94 [0.93, 0.94]	0.96 [0.96, 0.96]
Green	0.91 [0.90, 0.92]	0.88 [0.87, 0.89]	0.92 [0.91, 0.92]
Blue	0.91 [0.90, 0.92]	0.90 [0.89, 0.90]	0.93 [0.92, 0.93]
<b>Intraclass Correlation (ICC)</b>			
Red	0.95 [0.94, 0.96]	0.96 [0.96, 0.96]	0.94 [0.93, 0.94]
Green	0.91 [0.90, 0.92]	0.92 [0.91, 0.92]	0.88 [0.88, 0.89]
Blue	0.92 [0.90, 0.92]	0.93 [0.92, 0.93]	0.90 [0.89, 0.90]

\* N indicates number of observations.

\* The CCC and ICC were summarized with Median [Q1, Q3].

**Figure A. 1.** Cumulative percentage of the variance explained by the first 10 Principal Components.

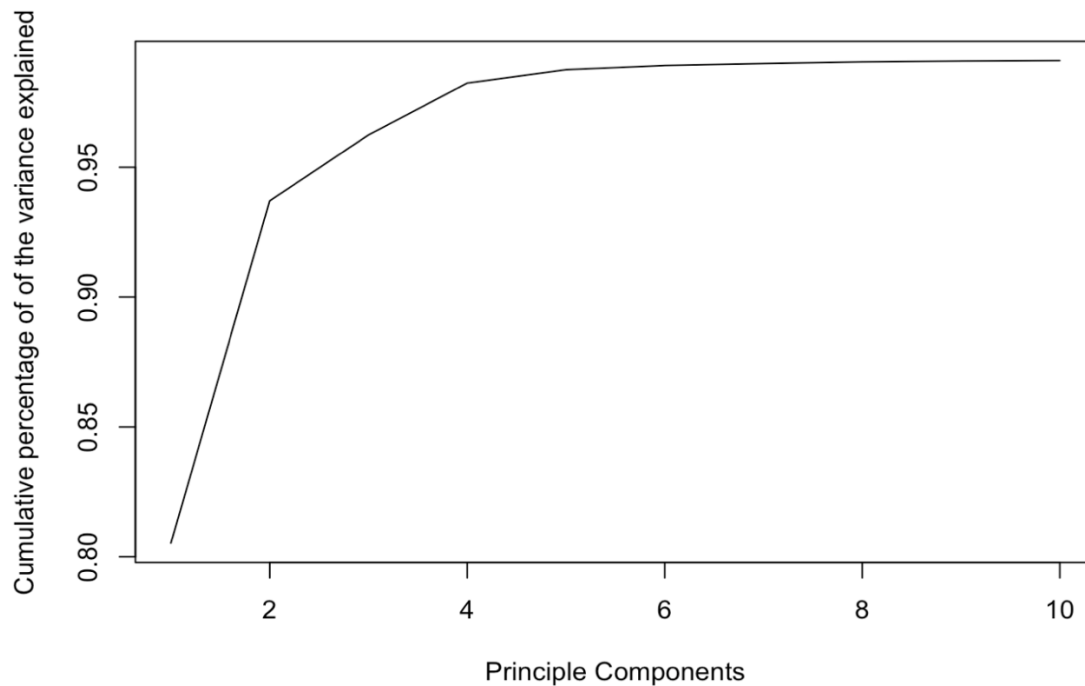
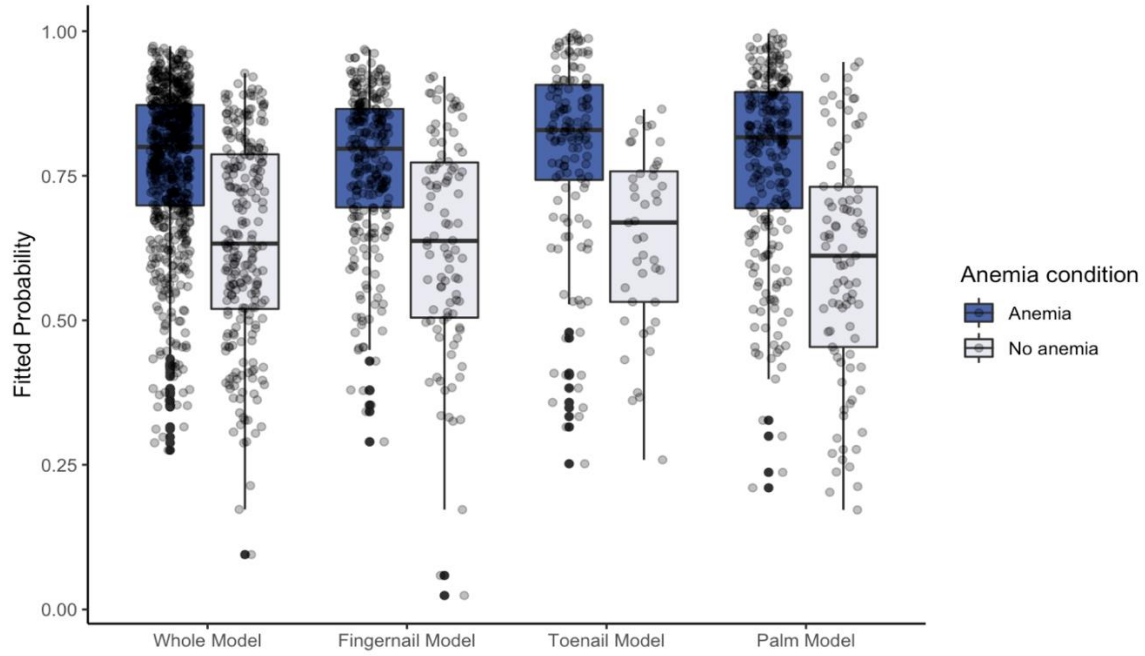


**Figure A. 2.** Evaluation of separating anemia and health group using predicted anemia probability.



## 7. Reference:

- [1]. Kalhan, M., Kaushal, P., Chayal, V., Verma, R., Singh, T., Yadav, G., Kumar, M., & Kumar, A. (2022). Prevalence of anemia among toddlers (12-36 months) in urban area of district Rohtak, Haryana. *Journal of family medicine and primary care*, 11(6), 2532–2536.  
[https://doi.org/10.4103/jfmmpc.jfmmpc\\_1469\\_21](https://doi.org/10.4103/jfmmpc.jfmmpc_1469_21)
- [2]. Allali, S., Brousse, V., Sacri, A. S., Chalumeau, M., & de Montalembert, M. (2017). Anemia in children: prevalence, causes, diagnostic work-up, and long-term consequences. *Expert review of hematology*, 10(11), 1023–1028. <https://doi.org/10.1080/17474086.2017.1354696>
- [3]. Widness J. A. (2008). Pathophysiology of Anemia During the Neonatal Period, Including Anemia of Prematurity. *NeoReviews*, 9(11), e520. <https://doi.org/10.1542/neo.9-11-e520>
- [4]. Persad, E., Sibrecht, G., Ringsten, M., Karlelid, S., Romantsik, O., Ulinder, T., Borges do Nascimento, I. J., Björklund, M., Arno, A., & Bruschetti, M. (2021). Interventions to minimize blood loss in very preterm infants-A systematic review and meta-analysis. *PloS one*, 16(2), e0246353. <https://doi.org/10.1371/journal.pone.0246353>
- [5]. De Ridder, B., Van Rompaey, B., Kampen, J. K., Haine, S., & Dilles, T. (2018). Smartphone Apps Using Photoplethysmography for Heart Rate Monitoring: Meta-Analysis. *JMIR cardio*, 2(1), e4. <https://doi.org/10.2196/cardio.8802>
- [6]. Gan, S.KE., Koshy, C., Nguyen, PV. et al. (2016). An overview of clinically and healthcare related apps in Google and Apple app stores: connecting patients, drugs, and clinicians. *Sci Phone Appl Mob Devices* 2, 8. <https://doi.org/10.1186/s41070-016-0012-7>
- [7]. Edward Jay Wang, William Li, Doug Hawkins, Terry Gernsheimer, Colette Norby-Slycord, and Shwetak N. Patel. (2016). HemaApp: noninvasive blood screening of hemoglobin using smartphone cameras. In *Proceedings of the 2016 ACM International Joint Conference on*



Pervasive and Ubiquitous Computing (UbiComp '16). Association for Computing Machinery, New York, NY, USA, 593–604. <https://doi.org/10.1145/2971648.2971653>

[8]. Mannino, R. G., Myers, D. R., Tyburski, E. A., Caruso, C., Boudreaux, J., Leong, T., Clifford, G. D., & Lam, W. A. (2018). Smartphone app for non-invasive detection of anemia using only patient-sourced photos. *Nature communications*, 9(1), 4924. <https://doi.org/10.1038/s41467-018-07262-2>

[9]. Pagana, K. D., Pagana, T. J., & Pagana, T. N. (2021). *Mosby's Diagnostic and Laboratory Test Reference*. Elsevier.

[10]. Sheth, T. N., Choudhry, N. K., Bowes, M., & Detsky, A. S. (1997). The relation of conjunctival pallor to the presence of anemia. *Journal of general internal medicine*, 12(2), 102–106. <https://doi.org/10.1046/j.1525-1497.1997.00014.x>

[11]. Hasanbegovic, E., Cengic, N., Hasanbegovic, S., Heljic, J., Lutolli, I., & Begic, E. (2016). Evaluation and Treatment of Anemia in Premature Infants. *Medical archives (Sarajevo, Bosnia and Herzegovina)*, 70(6), 408–412. <https://doi.org/10.5455/medarh.2016.70.408-412>